



Published in final edited form as:

*J Neurosci Methods*. 2010 August 15; 191(1): 90–93. doi:10.1016/j.jneumeth.2010.05.019.

## High-Throughput Study of Synaptic Transmission at the Neuromuscular Junction Enabled by Optogenetics and Microfluidics

Jeffrey N. Stirman<sup>a</sup>, Martin Brauner<sup>b</sup>, Alexander Gottschalk<sup>b,c</sup>, and Hang Lu<sup>\*,a,d</sup>

<sup>a</sup>School of Chemical and Biomolecular Engineering, Georgia Institute of Technology, 311 Ferst Drive, Atlanta, GA, USA

<sup>b</sup>Johann Wolfgang Goethe-University Frankfurt Institute of Biochemistry, Biocenter N220, Max-von-Laue-Str. 9, D-60438, Frankfurt, Germany

<sup>c</sup>Frankfurt Molecular Life Sciences Institute (FMLS), Johann Wolfgang Goethe-University, Max-von-Laue-Str. 9, D-60438 Frankfurt, Germany

<sup>d</sup>Interdisciplinary Program in Bioengineering, Institute of Biosciences and Bioengineering, Georgia Institute of Technology, Atlanta, GA, USA

### Abstract

Over the past several years, optogenetic techniques have become widely used to help elucidate a variety of neuroscience problems. The unique optical control of neurons within a variety of organisms provided by optogenetics allows researchers to probe neural circuits and investigate neuronal function in a highly specific and controllable fashion. Recently, optogenetic techniques have been introduced to investigate synaptic transmission in the nematode *Caenorhabditis elegans*. For synaptic transmission studies, although quantitative, this technique is manual and very low-throughput. As it is, it is difficult to apply this technique to genetic studies. In this paper, we enhance this new tool by combining it with microfluidics technology and computer automation. This allows us to increase the assay throughput by several orders of magnitude as compared to the current standard approach, as well as improving standardization and consistency in data gathering. We also demonstrate the ability to infuse drugs to worms during optogenetic experiments using microfluidics. Together, these technologies will enable high-throughput genetic studies such as those of synaptic function.

### Keywords

microfluidics; optogenetics; *C. elegans*; synaptic function; channelrhodopsin

## 1. Introduction

In the last few years, a large number of researchers have begun to use the light-activated Channelrhodopsin-2 (ChR2) as a method of neural stimulation. This research includes

© 2010 Elsevier B.V. All rights reserved.

\*hang.lu@gatech.edu; Tel: +1-404-894-8473; Fax: +1-404-894-4200.

**Publisher's Disclaimer:** This is a PDF file of an unedited manuscript that has been accepted for publication. As a service to our customers we are providing this early version of the manuscript. The manuscript will undergo copyediting, typesetting, and review of the resulting proof before it is published in its final citable form. Please note that during the production process errors may be discovered which could affect the content, and all legal disclaimers that apply to the journal pertain.

mapping of synaptic connectivity in mice (Wang et al., 2007), dissecting neuronal circuitry in brains with Parkinsons disease (Gradinaru et al., 2009), examining the escape response in zebrafish (Douglass et al., 2008), and examining mechanosensory and avoidance circuits in *C. elegans* (Guo et al., 2009; Nagel et al., 2005). Recently, we have used ChR2 to examine synaptic transmission in *Caenorhabditis elegans* (*C. elegans*) - a technique termed optogenetic investigation of neurotransmission (OptIoN) (Liewald et al., 2008). In this technique, behavioural changes in *C. elegans* (relative changes in body length) are induced by muscle contractions or relaxation caused by excitatory or inhibitory signals from either cholinergic or GABAergic motoneurons expressing ChR2 respectively, which are stimulated by blue light illumination. Defects in synaptic transmission alter this behavioural output and can therefore be observed and quantified. To do this, individual worms (wild-type or mutant) are picked onto plates. A video of the worm is then recorded under no illumination and blue light illumination, which is manually moved to track the worm as it moves. Finally the videos are analysed only semi-automatically (identifying the centre-line of the animal and measuring the length) to compare mutants to wildtype worms to infer functions of genes. Besides being manual, an additional problem with this approach is that photo-stimulation of cholinergic cells causes animals to coil, due to co-stimulation of GABAergic neurons via cholinergic input. The coiling causes significant problems in image processing and length determination. Although already a powerful new technique, OptIoN's current drawbacks of low throughput, manual manipulation of animals, variation in animal analysis and long data processing time need to be overcome to make it a widely applicable tool in neurogenetics.

Here, we combine the ChR2 technology with microfluidics and automated image processing for high-throughput, non-biased, and well-controlled experimentation to study synaptic transmission in large numbers of animals. Microfluidics when combined with automated image processing has been shown to greatly increase the speed and efficiency of handling, imaging, analysis, and sorting of cells and small organisms like *C. elegans* (Chung et al., 2008; Crane et al., 2009; Hulme et al., 2010; Hung et al., 2005; Rowat et al., 2009).

## 2. Materials and Methods

### 2.1 *C. elegans* culture

All worm strains used in this study were grown at 22 °C in the dark on standard nematode growth medium (NGM) plates with OP50 bacteria. All-*trans* retinal (ATR) is a required cofactor for channelrhodopsin and must be supplemented to *C. elegans* in order to have active channelrhodopsin. Those experiments using plates containing ATR (Sigma-Aldrich) were made by diluting a 50 mM stock ATR solution (in ethanol) in 300 µl OP50 to a final concentration of 100 µM and spreading on a 5.5 cm NGM plate. All animals tested were F1 progeny of P0 adults picked onto ATR or no-ATR plates 3.5 days prior to experiments. The strains used in this paper include ZX426: N2; *zxls3[punc-47::chop-2(H134R)::yfp; lin-15+]*, ZX460: N2; *zxls6[punc-17::chop-2(H134R)::yfp; lin-15+]* and ZX497: *unc-49(e407); zxls6*.

### 2.2 Microfluidic Device Design, Fabrication, and Operation

To achieve the high throughput in a controllable integrated system, we designed and fabricated a two-layer polydimethylsiloxane (PDMS, Dow-Corning) device using multi-layer soft lithography (Unger et al., 2000). The device is composed of eight parallel imaging channels connecting a loading and an un-loading chamber. These channels can be isolated (trapping the worm) by actuating a set of two valves (Valve 1 and Valve 2) (Fig. 1a). The main imaging channels are 60 µm wide: slightly larger than the width of a young adult worm. The cross-sections of the valves are rectangular and are therefore only partially

closed, allowing some fluid flow (as well as very young worms) while preventing larger animals to pass through the channels. We chose to use a single large valve, which covers all channels, instead of eight individual valves. This greatly simplifies the device construction, set-up, and operation. To aid in downstream image processing, we filled the valve channels with a 58% glycerol solution. This solution has a refractive index closely matching that of PDMS; at the location where a valve channel crosses a flow channel, only a faintly contrasting line is seen, a dramatic improvement from when the valve channel is filled with air or water.

To operate the device, initially Valve 1 is closed and Valve 2 is open. Worms are pushed into the device by pressure-driven flow, and are stopped at Valve 1. The pressure drop due to a loaded worm diverts additional worms to unloaded channels (Supplemental Video 1 online). When worms have filled the channels, Valve 2 is closed and the driving fluid pressure is turned off. After the completion of the illumination cycle, fluid pressure is turned back on and Valve 1 is opened flushing the animals from the imaging area. Valve 1 is then closed and Valve 2 opened beginning another cycle.

For the infusion of soluble drugs, a 20 gauge stainless steel hypodermic tubing Y connector (SmallParts) was used in the inlet. After introducing the worms into the device through one inlet of the Y, the inlet was closed with an off chip pinch valve (Cole Parmer) and a 30 mM solution of nicotine (Sigma-Aldrich) was introduced through the other inlet of the Y ( $t = 1$  second).

### 2.3 Image Acquisition and Analysis

All experiments were performed on a Leica DM IRB inverted microscope with a 4 $\times$  objective and a Hamamatsu Orca camera. Custom software was written in LabVIEW 8.5 with Vision to control worm injection, valve actuation, and video acquisition. Blue light illumination ( $0.3 \text{ mW/mm}^2$ ) was delivered via the epi-fluorescent port from a Leica EL6000 metal-halide fluorescent light source, filtered through a GFP excitation filter (450–490 nm) and electronically shuttered. The microscope was properly aligned for Koehler illumination insuring even blue illumination across the entire field of view. On-chip valves were controlled by the computer through off-chip Hargraves valves. After loading and isolating the worms, a movie was started (8 f/s at  $1280 \times 1024$ ) with no blue light illumination to obtain a baseline reading of the worms' lengths (Fig. 1c). After 2 seconds, the shutter was opened to illuminate the worms for another 5 seconds (Fig. 1d), after which time the shutter was closed. Then the worms were unloaded and another cycle begun. A video showing worms loading, light-induced contraction, and unloading can be found in the ESI.

These movies were post-processed using custom software written in LabVIEW. Movies were analyzed frame-by-frame, first identifying each of the eight channels (Fig. 1c,d; in this example the strain ZX497 was used), determining if the channel contains a single worm and isolating these channels (Fig. 1e,f) (discarding channels if they contain zero or multiple worms). These isolated images were then processed to identify the worm (filtering out the edges of the channel) and threshold, and finally the worm was thinned to a single pixel backbone (Stephens et al., 2008) (Fig. 1g,h). For each animal the length of a spline fit to this backbone was then measured and these lengths were normalized to the average length during the two second time interval prior to blue-light illumination. Finally, at each time point the average of all relative body lengths of a particular strain was calculated and plotted as a function of time (Fig. 2a). Comparisons of the mean relative body lengths can be made between wild-type animals and those with mutations in genes involved in synaptic transmission (Fig. 2b). Only those animals of stage L4 to adults (based on length) were included in the analysis and animals not meeting these criteria were rejected (e.g. the second channel from top in Fig. 1c,d).

### 3. Results and Discussions

We successfully designed and fabricated the microfluidic devices, and integrated with the off-chip hardware and the control/image analysis software. The microfluidic chip design and operation features lead to a low occurrence in which there is more than one worm in a single channel (<5%) (Fig. 1b). Loading, isolation, and release time averaged 13 seconds, and after worm isolation, our experiments lasted 7 seconds (2 seconds with no illumination and 5 seconds with blue illumination). This averages to 3 loading cycles per minute and an average of ~6.6 single worms per loading cycle (Fig. 1b), yielding an over-all rate of about ~20 animals per minute. The experimental loading efficiency depends on a number of factors, including worm density and driving fluidic pressure. There is a trade-off between the number of channels with single worms versus multiple worms and the loading time and loading efficiency. We have previously found (Liewald et al., 2008) that due to both population heterogeneity and image processing uncertainty, roughly 20–50 worms per strain are needed to get a reliable and statistically significant measurement of the population averaged length. While further optimization in manual methods is possible, it would involve picking a number of animals into the field of view of the camera. It would be quite challenging to get a number of animals into an area (roughly  $2.5 \times 3.5$  mm) and preventing them from crawling away during the experimental time. Furthermore, this also emphasizes the necessary human manipulation for the manual method, which is cumbersome and not easily reproduced. Though slight increases in the field of view are also possible, only minimal gains can be made before the requisite resolution of the system is lost (about  $3 \mu\text{m}$ /pixel). Based on the measured throughput of our system, the rate of processing animals is already two orders of magnitude faster than manual approaches.

We tested wild-type and mutant nematodes expressing ChR2 in the motor neurons innervating the body-wall muscles. One set of animals (strain ZX426) carried *zxIs3*, a transgene encoding ChR2 in the GABAergic neurons which act to release an inhibitory transmitter (White et al., 1986) at the neuromuscular junction (NMJ) of body-wall muscle cells. Upon blue light excitation, GABA released from these neurons into the NMJ synaptic cleft binds to GABA<sub>A</sub> receptors on the muscle cell, leading to a hyperpolarization and thus relaxation of the muscle. This can be seen as a lengthening of the animal's body (Fig. 2a, b). *zxIs6* is a transgene causing expression of ChR2 in the cholinergic neurons, which act in an excitatory fashion (White et al., 1986) at the NMJ (strain ZX460). When *zxIs6* worms are exposed to blue light, a shortening of the animal is observed (Fig. 2a, b) due to the release of acetylcholine, which induces muscle depolarization and thus contraction. Animals mutant in the *unc-49* gene (encoding the GABA<sub>A</sub> receptor) carrying the *zxIs6* transgene showed an additional decrease in body length (Fig. 2a, b) under blue light illumination (strain ZX497). This is because the cholinergic motor neurons connect to GABAergic neurons, such that GABA release is co-activated by ACh release, which reduces the activating effect of ACh (unless the UNC-49 GABA<sub>A</sub>R is absent). The data in Fig. 2a, b agree extremely well with those we previously obtained by standard manual methods (Liewald et al., 2008). This demonstrates that the microfluidic devices coupled with the automation and image processing tools give comparable experimental results, but are faster and more easily standardized.

An additional advantage of using the microfluidic setup is the ability to infuse drugs during experiments. To demonstrate the utility of this microfluidic chip, we combined the stimulation of the neurons with ChR2 along with exposure of the animal to a soluble drug. Nicotine is a known acetylcholine receptor agonist (present on the muscle cells at the NMJ) that causes a depolarization (and thus contraction) of the muscle cells (Richmond and Jorgensen, 1999). The microfluidic device was used to deliver M9 buffer containing nicotine to *zxIs3* worms; this strain relaxes under blue light illumination. Within seconds of the

nicotine stimulation, the worms began to contract (Fig. 2c) ( $n = 49$ ), rapidly at first and then gradually slowing. At  $t = 180$  seconds, the blue light was turned on to excite the GABAergic neurons, releasing the neurotransmitter GABA into the neuromuscular junction. This led to a hyper-polarization of the muscle cells, as seen in the increase in the worms' lengths (relaxation of the muscles), which then decreased rapidly because of the continued presence of nicotine. This additional ability to perfuse drugs adds to the toolbox for these types of studies.

## 4. Conclusions

In general, based on our loading efficiency and animal processing time, we can gather data from about 100 individual animals in less than 5 minutes, and therefore can test animals a couple of orders of magnitude faster than conventional methods. It is conceivable to further increase this throughput by denser packing of the channels or increasing the field of view. An additional benefit of confining the worms to channels within the chip is the reduction in the amount of freedom in movement the worms have, while still allowing the relaxation and extension of the body wall muscles unimpeded, which is important in this type of analysis. In restricting the environment of the worm in the microfluidic chip, we prevent the worms from coiling on themselves, and this greatly facilitates the image processing steps. Microfluidic technology also allows us to accurately and repeatedly deliver soluble compounds, which is not possible in off chip assays. In the longer term, this technology can be used to automate screening of a large number of different populations for a variety of applications such as studying synaptic transmission.

## Supplementary Material

Refer to Web version on PubMed Central for supplementary material.

## Acknowledgments

The authors acknowledge US National Science Foundation (DBI-0649833 to HL) and National Institutes of Health (NS058465 to HL) as well as the Deutsche Forschungsgemeinschaft (GO1011/2-1 and Cluster of Excellence Frankfurt – Macromolecular Complexes, to AG) for funding. HL is a DuPont Young Professor and a Sloan Research Fellow.

## References

- Chung KH, Crane MM, Lu H. Automated on-chip rapid microscopy, phenotyping and sorting of *C. elegans*. *Nat. Methods*. 2008; 5:637–643. [PubMed: 18568029]
- Crane MM, Chung K, Lu H. Computer-enhanced high-throughput genetic screens of *C. elegans* in a microfluidic system. *Lab on a Chip*. 2009; 9:38–40. [PubMed: 19209332]
- Douglass AD, Kraves S, Deisseroth K, Schier AF, Engert F. Escape behavior elicited by single, Channelrhodopsin-2-evoked spikes in zebrafish somatosensory neurons. *Curr Biol*. 2008; 18:1133–1137. [PubMed: 18682213]
- Gradinaru V, Mogri M, Thompson KR, Henderson JM, Deisseroth K. Optical Deconstruction of Parkinsonian Neural Circuitry. *Science*. 2009; 324:354–359. [PubMed: 19299587]
- Guo ZV, Hart AC, Ramanathan S. Optical interrogation of neural circuits in *Caenorhabditis elegans*. *Nat. Methods*. 2009; 6 891-U47.
- Hulme SE, Shevkopyas SS, McGuigan AP, Apfeld J, Fontana W, Whitesides GM. Lifespan-on-a-chip: microfluidic chambers for performing lifelong observation of *C. elegans*. *Lab on a Chip*. 2010; 10:589–597. [PubMed: 20162234]
- Hung PJ, Lee PJ, Sabounchi P, Lin R, Lee LP. Continuous perfusion microfluidic cell culture array for high-throughput cell-based assays. *Biotechnology and Bioengineering*. 2005; 89:1–8. [PubMed: 15580587]

- Liewald JF, Brauner M, Stephens GJ, Bouhours M, Schultheis C, Zhen M, Gottschalk A. Optogenetic analysis of synaptic function. *Nat Methods*. 2008; 5:895–902. [PubMed: 18794862]
- Nagel G, Brauner M, Liewald JF, Adeishvili N, Bamberg E, Gottschalk A. Light activation of channelrhodopsin-2 in excitable cells of *Caenorhabditis elegans* triggers rapid behavioral responses. *Current Biology*. 2005; 15:2279–2284. [PubMed: 16360690]
- Richmond JE, Jorgensen EM. One GABA and two acetylcholine receptors function at the *C-elegans* neuromuscular junction. *Nature Neuroscience*. 1999; 2:791–797.
- Rowat AC, Bird JC, Agresti JJ, Rando OJ, Weitz DA. Tracking lineages of single cells in lines using a microfluidic device. *Proceedings of the National Academy of Sciences of the United States of America*. 2009; 106:18149–18154. [PubMed: 19826080]
- Stephens GJ, Johnson-Kerner B, Bialek W, Ryu WS. Dimensionality and dynamics in the Behavior of *C-elegans*. *Plos Computational Biology*. 2008; 4
- Unger MA, Chou HP, Thorsen T, Scherer A, Quake SR. Monolithic microfabricated valves and pumps by multilayer soft lithography. *Science*. 2000; 288:113–116. [PubMed: 10753110]
- Wang H, Peca J, Matsuzaki M, Matsuzaki K, Noguchi J, Qiu L, Wang D, Zhangn F, Boyden E, Deisseroth K, Kasai H, Hall WC, Feng G, Augustine GJ. High-speed mapping of synaptic connectivity using photostimulation in Channel rhodopsin-2 transgenic mice. *Proceedings of the National Academy of Sciences of the United States of America*. 2007; 104:8143–8148. [PubMed: 17483470]
- White JG, Southgate E, Thomson JN, Brenner S. The Structure of the Nervous-System of the Nematode *Caenorhabditis-Elegans*. *Philosophical Transactions of the Royal Society of London Series B-Biological Sciences*. 1986; 314:1–340.



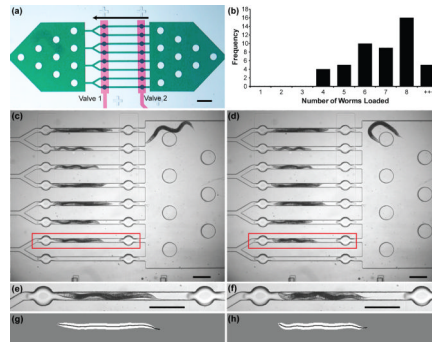


**Fig. 1.** Microfluidic chip greatly increases the speed of animal handling and sample processing. (a) Microfluidic device for parallel investigation of *C. elegans* responses to light stimulation. Green channels are in the flow layer (where *C. elegans* are located) and the red channels are in the valve control layer. Arrow indicates direction of worm loading. Scale bar is 500  $\mu\text{m}$ . (b) Histogram of the worm loading efficiency. Channels with zero or multiple worms (column +++) were not analyzed. We found an average of  $\sim 6.6$  worms could be analyzed per loading cycle. (c)–(h) Schematics of computer data processing. Worm strain in this image is ZX497, expressing ChR2 in the cholinergic neurons in an *unc-49(e407)* background;. (c) Bright field image of loaded worms prior to blue light illumination. (d) Bright field image of loaded worms 2 seconds after turning on blue light illumination. These animals show body length shortening due to muscle contraction. The analysis program identifies each channel (red box) and separates it for further processing. (e), (f) Zoom-in view of the areas selected by the red boxes. (g), (h) For each channel section, the worm is first identified and separated from the rest of the image, and then thresholded (white). Then a curve (black) is fit to the midline of the animal and its length is measured. This process is done for every frame of the movie (8 fps). From this length data the curves in Fig. 2a are generated. Scale bars are 250  $\mu\text{m}$ .

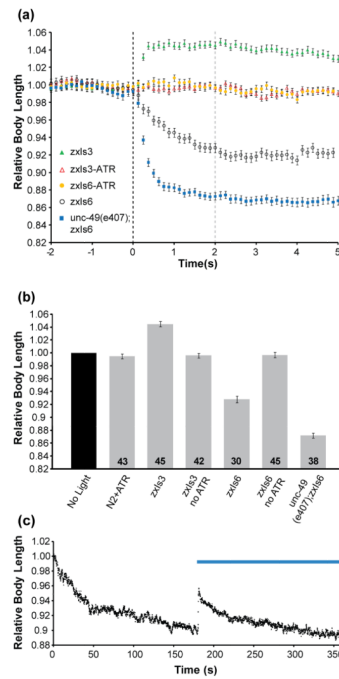


**Fig. 2.** Contraction and relaxation of *C. elegans* muscles under photoactivation of motor neurons. (a) Changes in body length over a 7-second interval. Body length for an individual animal is relative to an average of the body length of that animal captured over the 2 second interval prior to blue light illumination. Blue light was turned on at  $t = 0$ . (b) Mean relative body length (of the strain population) measured 2 seconds after continuous blue light illumination (indicated by the dashed gray line at  $t=2$  sec. in (a)). The numbers of individual animals tested are indicated at the bottom of the bars. (c) Nicotine (30 mM) induced contraction and ChR2 induced relaxation ( $n = 49$ ). Blue bar indicates time when blue light illumination is present. ATR was added to the growth media to yield functional ChR2, unless otherwise indicated. Error bars are s.e.m.